Space Charge and Dead Zone Analysis in the TWIST Spectrometer

Brynle Barrett
TRIUMF Summer Student
Saint Mary's University

August 27, 2004

Contents

List of Figures

List of Tables

Abstract

Multi-wire chamber ionization detectors experience effects from space charges due to high energy loss of the radiative particles that penetrate them. One of these effects is that of the dead zone. A thorough study has been done on the dead zone produced by μ^+ in the proportional counters closest to the target stop in the TWIST spectrometer, PC5 and PC6. Emphasis is placed on the method of analysis and the results found in raw data.

The length of the dead zone was found to be $L_{dead} = 0.2630 \pm 0.0117$ cm in PC5, and $L_{dead} = 0.4811 \pm 0.0050$ cm in PC6. The lifetime for the dead zone to heal was found to be $\tau_h = 1856 \pm 82$ ns in PC5, and $\tau_h = 2444 \pm 41$ ns in PC6.

Monte Carlo results were not available, due to technical problems with the experiment simulation code. A brief description of the TWIST experiment and the physics of the dead zone are also given.

Chapter 1

Introduction

Throughout the course of the summer, under the supervision of Dr. Art Olin, I have been performing a study on space charge effects created by the M13 muon beamline in a proportional counter (PC6) inside the TWIST spectrometer. Here I will give a brief introduction to what a space charge is and how it effects measurements made by PC6 in the spectrometer.

1.1 Proportional Counters

A proportional counter is a type of wire chamber, and a wire chamber is a type of radiation detector. These types of detectors are constructed as shown in figure (1.1), with a plane of wires suspended between two planes of metalic foil which act as cathodes. When a negative voltage is applied to the foils a positive charge is induced on the anodes, creating an electric field governed by equation (1.1):

$$V(x,y) = -\frac{CV_o}{4\pi\epsilon} \ln\left[4\left(\sin^2\frac{\pi x}{s} + \sinh^2\frac{\pi y}{s}\right)\right] \tag{1.1}$$

Where:

- $V_o \rightarrow$ Applied voltage
- $\epsilon \rightarrow$ Dielectric constant of gas used
- $s \rightarrow$ Wire spacing
- $C \rightarrow$ Anode-cathode capacitance Also, if $d \ll s \ll L$ then:

$$C = \frac{2\pi\epsilon}{\frac{\pi L}{s} - \ln\left(\frac{\pi d}{s}\right)} \tag{1.2}$$

- $L \rightarrow$ Anode-cathode gap
- $d \rightarrow$ Wire diameter

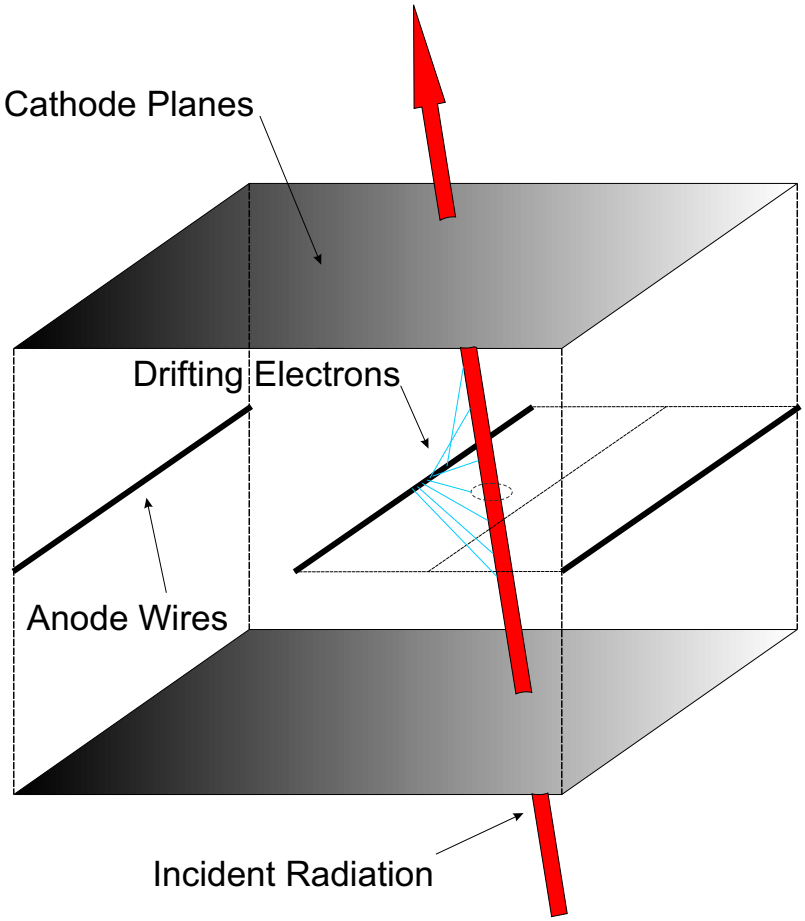

Figure 1.1: Multi-Wire Proportional Chamber

The chamber is filled with a neutral gas, like a Noble gas, at constant pressure to interact with incident radiation which creates an electron-ion pair. The electron and ion are then accelerated to the anode and cathode respectively. The electron moves with greater mobility then the positively charged ion, since it is much lighter. Once it is within a few wire radii of the wire, it begins to accelerate with enough energy to create another electron-ion pair, should it collide with a gas molecule. The secondary electron does the same thing, and so on, producing an avalanche of electron-ions pairs. This avalanche forms a tear drop shape of positive and negative charges as it moves, with mostly electrons at the head, and positive ions at the tail.

The negative charge is collected by the anode wires, while the positively charged ions drift back to the cathode. It is this positive charge drift that induces a current in the anode wires and forms a sharp negative voltage pulse. This pulse is then analyzed by Time to Digital Converters (TDC's) which are used to 'detect' the incident radiation.

One might ask why it is not the electrons that induce the pulse. They are, afterall, moving a lot faster towards the anode wire than the ions are moving back to the cathode plane. It is because of the sequential charge pairs that are created in the avalanche. Each pair, on its own, contributes a net charge of zero in a region surrounding it; therefore little or no charge is induced by the electrons *drifting*. However, it can be shown that there is a small effect due to the *collection* of electrons by the anode wire. A small current due to this electron collection is produced, which essentially governs the rise time of the signal pulse. It is the positive ion drift back to the cathode that continues the tail of the pulse. This tail is much longer in duration then the rise time. It is the part of the signal most measured.

Moreover, proportional counters work in the voltage range of about $200 \rightarrow 600$ V. In this range the amount of amplified current produced is proportional to the initial number of electron-ion pairs created. So the signal strength (or length of duration) is proportional to the energy deposited in the gas by the incident radiation.

Additional information can be found using these detectors. The position at which the radiation passed through the detector can be approximated by the position of the wire: $x \pm s/2$. Since the same signal can be produced on either side of the wire there is a left-right ambiguity.

However, only *one* position coordinate can be found per wire plane, since the wire planes are only sensitive to the direction perpendicular to which they run. To get the y-coordinate another plane of wires is needed at a different z-value, this time with wires running perpendicular to the plane next to it.

1.2 Drift Chambers

Similar to PCs, drift chambers (DCs) use the ionization of neutral gas molecules to detect the position of an event. The difference between DCs from PCs is that their cells are filled with a *slower* gas, that is the time for the ions to drift back to the cathode from the anode wire is much larger than the PCs. The spacing between the cathode and anode wire is also larger, further lengthening the drift time. The purpose of this is to more accurately calculate the position of the event inside the wire chamber cell.

But because of the left-right ambiguity, many hits to the same track must be used to resolve which side (the left or the right) of the wire the hit was most likely to orginate.

1.3 The TWIST Spectrometer

The TWIST Spectrometer consists of a superconducting solenoid magnet, which produces a close to uniform 2 tesla magnetic field. The M13 beamline is fired down the center of the solenoid, along the positive z-direction. This is the source of muons needed for the experiment, whose goal is to measure the four Michel parameters (ρ, η, δ, and ξ) which are related to the weak interaction occurring in positive muon decay. By finding the four Michel parameters to a greater precision then ever before measured, the TWIST experiment will be able to observe any deviations in reality from the standard model. But its result, in the end, may be limited my systematic uncertainties. The purpose of this study is therefore aimed at finding the systematic uncertainty due to dead zones in the TWIST spectrometer.

The spectrometer is designed such that incident muons travel through the upstream half of the spectrometer then decay in a target located at $z = 0.0$ cm. A muon decays into a positron, an electron neutrino and a muon anti-neutrino as illustrated in figure (1.2). Once decayed, the positron creates tracks in the wire chambers which could be in the upstream or downstream chambers.

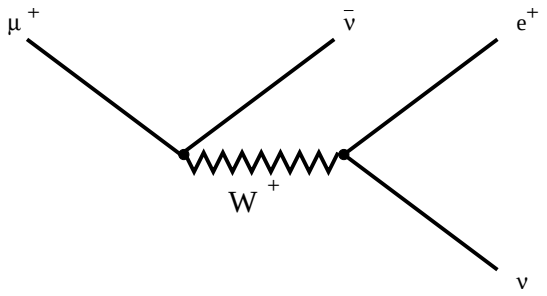

Figure 1.2: Feynman Diagram of $\mu^+ \rightarrow e^+ + \bar{\nu}_\mu + \nu_e$

As shown in figure (1.3), inside the solenoid are 56 planes of wire chambers, each oriented in a particular direction in order to measure the positions of muon and positron tracks. There are two types of wire chambers in the spectrometer: Proportional Counters (PCs) and Drift Chambers (DCs). They both serve a different purpose.

The DCs are placed near the center of the upstream and downstream chambers. They have a *slow* gas; ie, the ions take longer to drift back to the cathode. This makes the

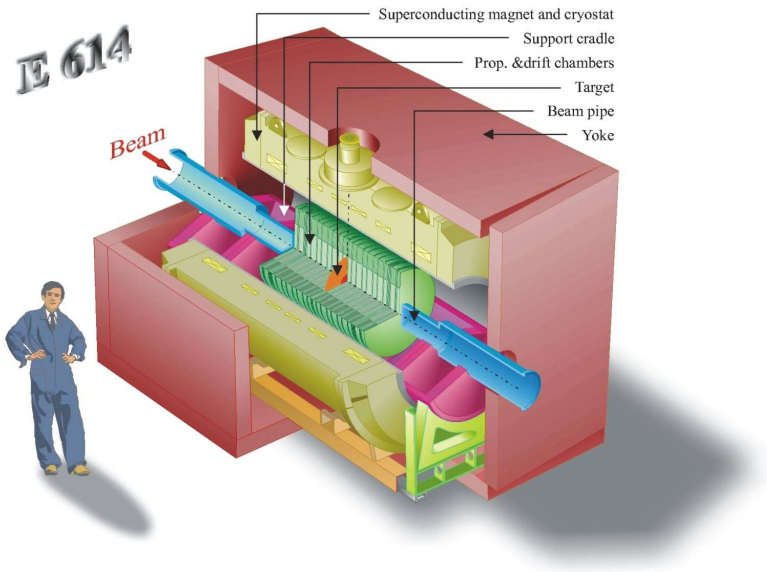

Figure 1.3: TWIST Spectrometer

width of the pulses much longer then the PCs, thus giving a more precise measurement of the drift time due to the limitations of electronics. These time measurements give a more precise measurement of the positions at which the events occured. The improved positions are then used for the least squares helix fitting of the positron tracks in both the upstream and downstream chambers.

Recall that in a uniform magnetic field along the z-axis the equation of motion of a charged particle is a helix, and the most general form is given by equations (1.3) $\rightarrow$ (1.5):

$$x(z) = x_o + \frac{p_{y_o}}{qB_z}\left[\frac{1}{\sin\varphi}\sin\left(\frac{qB_z}{p_z}(z-z_o)-\varphi\right)+1\right] \tag{1.3}$$

$$y(z) = y_o + \frac{p_{x_o}}{qB_z}\left[\frac{1}{\cos\varphi}\cos\left(\frac{qB_z}{p_z}(z-z_o)-\varphi\right)-1\right] \tag{1.4}$$

$$z(z) = z \tag{1.5}$$

Where x_o, y_o, p_{x_o}, p_{y_o} and φ are determined by the initial conditions:

$$\begin{aligned} x(z_o) &= x_o \\ y(z_o) &= y_o \\ z(z_o) &= z_o \\ p_x(z_o) &= p_{x_o} \end{aligned}$$

$$p_y(z_o) \quad = \quad p_{y_o}$$

And $p_z(z) = \text{constant} \equiv p_z$.

The PCs are used for fast timing measurements, and are located at the entrance and exit of both upstream and downstream chambers. They contain a *fast* gas; ie, the ions drift back to the cathode relatively quickly, enabling small time scale measurements. These are needed for obtaining the start and end times of the muon and positron tracks. If no start or end times are available, there could not be a position calculation.

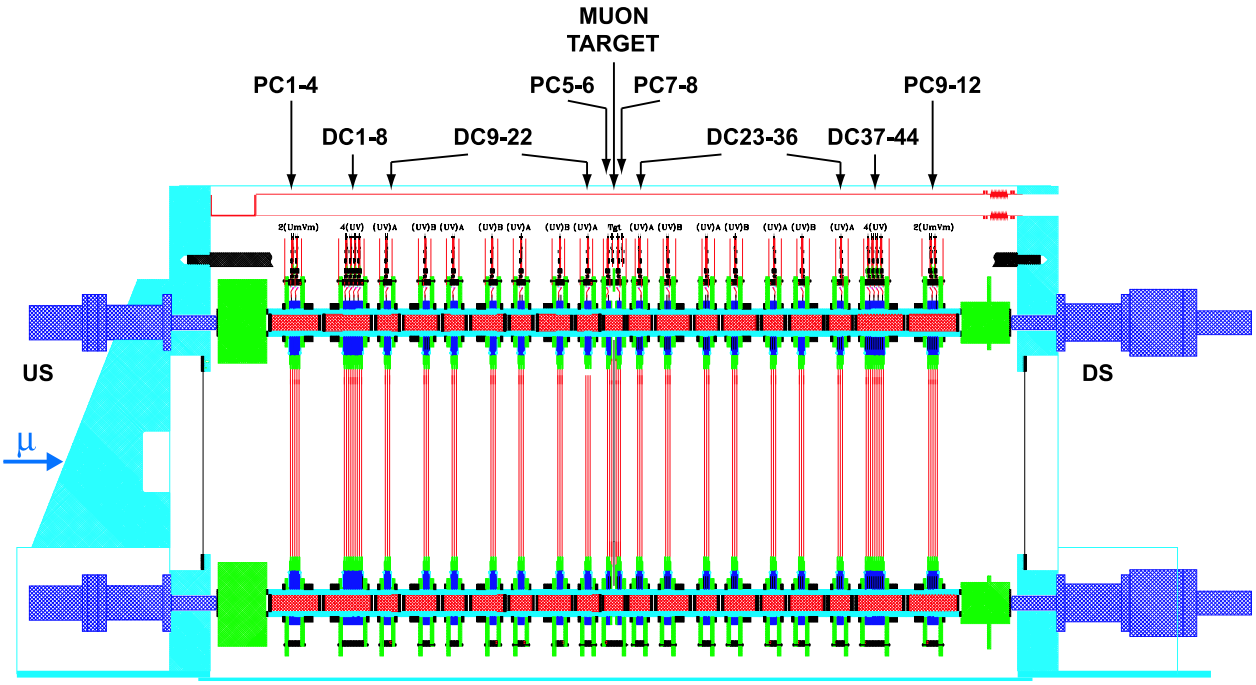

Figure 1.4: TWIST Spectrometer Side View

1.4 Space Charges and Dead Zones

Near the end of a muon track, before it decays, the muon deposits the most amount of energy in the gas. This relatively large deposit of energy forms many electron-ion pairs, each electron creating its own avalanche. Most of the ions are then created near the anode wire, where they must drift back towards the cathode. Such a large number of localized positive ions is what we call a *space charge* inside the wire chamber. This space charge has a finite decay time over which the ions recombine with electrons or drift back to the cathode.

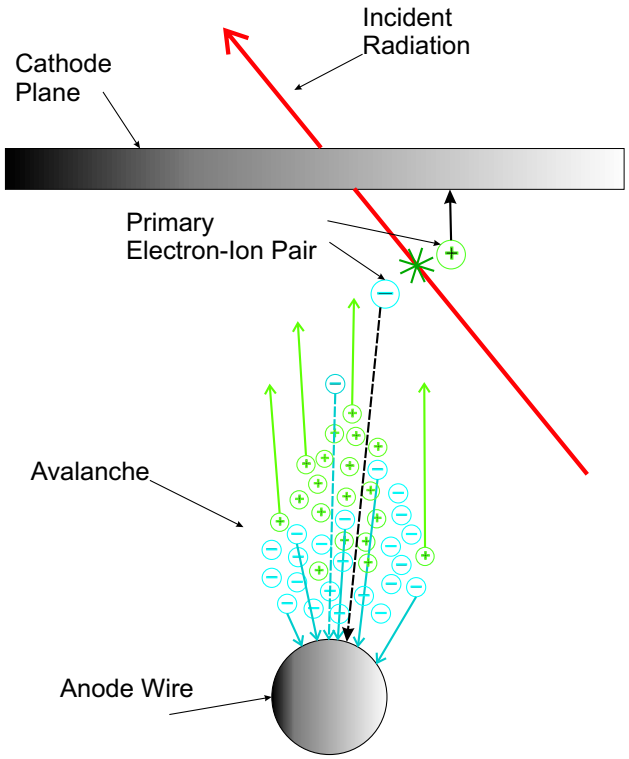

Figure 1.5: Avalanching Electrons in a Single Wire Chamber Cell

Suppose now that the positron decays upstream, back through the same region containing this space charge. In this case, any additional electron-ion pairs that are formed by the positron either recombine with the high density of positive ions that compose the space charge, or they are redirected away from the anode wire because the electric field has been destorted by the space charge. Without an electron-ion pair specific to that positron, no pulse is formed, and thus no position is recorded in the data. This region containing the space charge is what we call the *dead zone*, since the cells containing the wires act as if they are *dead*.

This study of the dead zone is, therefore, done mostly on PC5 and PC6, which are located nearest the muon target in the upstream chamber.

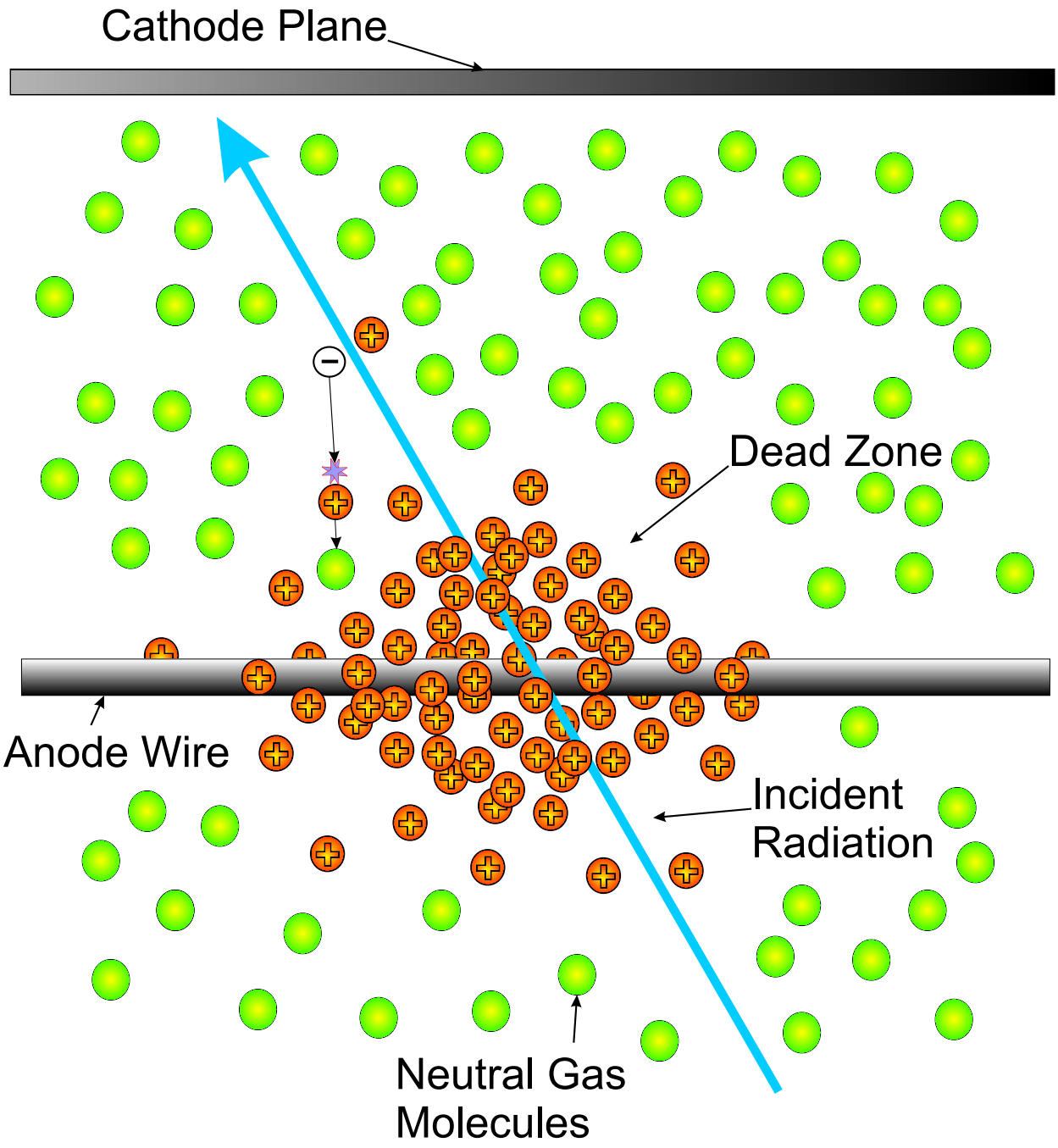

Figure 1.6: Effect of Dead Zone

Chapter 2

The Goal

The goal of this dead zone study is to answer the following questions:

(1) How large is the dead zone on average?

(2) How long does it take for the dead zone to "heal"?

(3) What is the probability that a positron will go through the dead zone without firing the corresponding wire?

(4) What effect does this dead zone have on the analysis of the Michel parameters? Ie; what is the systematic uncertainty of the dead zone effect?

With the help of Monte Carlo analysis using *GEANT3*, these questions can be answered. We began by first asking what data variables are needed to answer these questions and then writing a code that essentially fills different histograms, under the right conditions, that contain useful information.

As illustrated in this report, there are a number of checks we can perform to ensure our results are on track. One of them is to run the program on a set of Monte Carlo data and observe whether or not similar results are obtained.

The Monte Carlo simulation of the *TWIST* experiment is essential to this study. For example, we have no way of testing how large the dead zone is, or how long is lasts, without implementing specific numbers in *GEANT3*. If we can then get the same numbers back out that we had put in for the healing time τ_h and the dead length L_d, we know our analysis of the dead zone for raw data is correct.

Chapter 3

TWIST Software

The *TWIST* experiment is extremely dependent on its software. Most of its software is custom built, and requires fast computing power and vast memory banks to store the data and analysis results. In fact, the computing facilities at TRIUMF are insufficient for the jobs *TWIST* requires. So the experiment has applied and acquired high priority on the *WESTGRID* computing facility. This organization provides the CPUs for computing and storing data for many outside universities and organizations along the west coast.

There are two main processes the data must be run through in order to obtain the information needed for this study:

(1) *MOFIA* Analysis

MOFIA is the main analysis code. It takes the initial binary files that were created in sets during the first two years of data taking. The binary files contain all the raw data directly from the electronics connected to the *TWIST* spectrometer.

For each set of data (containing $\sim 2.5 \times 10^8$ events) there are about 200-300 runs that divide up the events. For each run *MOFIA* creates a `.root` file that contains histograms of different quantities, and different variables that are derived from the raw data.

So for each analyzed set, there are 200-300 files labeled: `treerun#.root` which need to be summed in order to get useful information. This is the next step.

(2) `ROOT` Tree Summing

ROOT is a very powerful object oriented physics analysis program that uses the C++ language as a platform. *TWIST* uses this software to conveniently store statistical information in a special `root` data structure called a *tree*.

`Root` trees are similar to directories, in that a single tree can contain many types of data structures. There are three main types of structures used by this experiment in the `root` trees:

(i) Histograms

(ii) Ntuples

(iii) Leaves

Histograms and Ntuples we know well, but what are leaves? Leaves are basically variables in array form that can be accessed in the same way as arrays or pointers passed as arguments in a function.

Leaves can even be histogramed under any numerical condition inside the `root` viewer by using its object oriented platform.

Using a code written by members of the *TWIST* group, the `root` run files in each analyzed data set can be summed over all the information in each file and reduce the analysis further to a single `.root` file.

Chapter 4

Analysis

Here is a brief description of the algorithm and method of analysis.

4.1 The Code

The bulk of the deadzone analysis is done by the set of subroutines I have attached to the end of Blair Jamieson's `HTree` analysis code. The following is a list of the code implemented in my version of `HTree`, found in:

`\home\bbarrett\Research`

(1) `HTree.C` and `HTree.h`

These are the implementation and header files of the main `HTree` analysis code. The last few lines contain the definitions of the subroutines I have written to perform the dead zone analysis called:

(i) `Deadzone()`

(ii) `DZComputHistos()`

(iii) `DZ_ErrorBars()`

(iv) `TH2D_Divide()`

(v) `TestTrackToZ()`

(2) `processhelixtrees`

Executable that performs `HTree` analysis.

(3) `trackswim.cpp` and `trackswim.h`

This code is just like it sounds, it "trackswims" a particle of charge q from and initial position (u, v, z) with momentum (p_u, p_v, p_z) in a uniform or non-uniform $\vec{B}$-field to a requested `ENDZ`. It then outputs the new coordinates (u, v,`ENDZ`) and momentum there.

(4) `magnet.cpp` and `magnet.h`

This code calculates the $\vec{B}$-field data: (B_u, B_v, B_z) at all neccessary (u, v, z) for the uniform or non-uniform cases, with the help of the internationally standardized magnetic field mapping program *OPERA*.

Once the data or Monte Carlo sets are run by the main analysis software *MOFIA*, the information is output into `.root` files in the form: `treerun#.root`. My code runs while the trees are summed, and outputs histograms that contain useful information about the dead zone.

4.2 The Geometry

The geometry of the spectrometer is crucial to understanding how to tackle this dead zone problem. As mentioned before, there are two types of wire chambers in the spectrometer: drift chambers and proportional counters. But where are each of these chambers located relative to the target stop at $z = 0$ cm? The following subsections give a very good description of this. Of couse, our problem only exists in the upstream (US) half of the spectrometer, so this is all the geometery data we need.

4.2.1 US Drift Chambers

There are a few parameters in the tables that follow which need explaining.

- The global plane numbers are simply plane numbers defined as the sequential order in which the muon would hit the planes if it went straight through the spectrometer.
- The z-coordinate is the distance, in cm, from the target stop.
- The rotation is the angle relative to horizontal at which the wire chambers are rotated.
- The instrumented wires per plane is the number of wires that are actually hooked up to counting electronics. We must also know that there are the same number of wires per

plane in any DC or PC. These wires that are not instrumented can still cause multiple scattering of the muon and positron. There are 80 wires per plane in any DC, where the wire spacing, $s = 0.4$ cm.

- The plane type depends on the angle of rotation. If the plane type is V, then the wires run along the U-direction and measure the v-coordinate of the tracks. If the plane type is U, then the wires run along the V-direction and measure the u-coordinate of the tracks.

Tables (4.1) and (4.2) were taken from: `/home/e614/e614soft/caldb_ascii/dt_geo.00038`

4.2.2 US Proportional Counters

The wire spacing, $s = 0.2$ cm for all PCs. Each one contains 160 wires per plane, but the last two in the US chamber only have 48 of those wires instrumented. All instrumented wires are located in the central region of the wire chambers, encompassing the muon beam spot.

4.3 The Algorithm

In order to extract information about the dead zone in the wire chamber of interest, we envoke the following algorithm:

- For each event:
  - For each window:
    - For the following criteria:
      (i) Event Type 1 (Simple Clean)
      (ii) Window Type 2 (Upstream Decay)
      (iii) $|\vec{P}_{tot}| \geq 20$ MeV
      (iv) $p_z \geq p_u$ (Where p_z is the momentum along the z-direction, and p_u is the momentum along the u-direction)
      (v) tolerance = ± 0.0980 cm (for PCs)
      tolerance = ± 0.1980 cm (for DCs)
      - Find the last (u, v) coordinates of the muon before it decays (requiring that the last v-plane hit is `pvlast_anal` and the last u-plane hit is

Global Plane #	Z (cm)	Rotation (°)	Instrumented Wires/Plane	Plane Type
5	-49.7929	-45.0	48	V
6	-49.3929	45.0	48	U
7	-48.9929	-45.0	48	V
8	-48.5929	45.0	48	U
9	-48.1929	45.0	48	U
10	-47.7929	-45.0	48	V
11	-47.3929	45.0	80	U
12	-46.9929	-45.0	80	V
13	-42.1933	45.0	80	U
14	-41.7933	-45.0	80	V
15	-34.9948	45.0	80	U
16	-34.5948	-45.0	80	V
17	-29.7950	45.0	80	U
18	-29.3950	-45.0	80	V
19	-22.5968	45.0	80	U
20	-22.1968	-45.0	80	V
21	-17.3975	45.0	80	U
22	-16.9975	-45.0	80	V
23	-10.1993	45.0	80	U
24	- 9.7993	-45.0	80	V
25	- 4.9997	45.0	80	U
26	- 4.5997	-45.0	80	V

Table 4.1: Geometry Data of Upstream DCs

`pulast_anal`). The (u, v) coordinates give us an approximate location of the dead zone.

- Does the upstream decay positron go back through the dead zone? If it did, then the (u, v) coordinates recorded in the data may or may not be from the planes we are analyzing. If the wire is dead when the positron passes by it, there can't be a recorded TDC signal from that particular wire. So we cannot simply use the data (u, v) in the data trees.

Global Plane #	z(cm)	Rotation (°)	Instrumented Wires / plane	Plane Type
1	-59.79	45.0	160	U
2	-59.39	- 45.0	160	V
3	-58.99	45.0	160	U
4	-58.59	- 45.0	160	V
27	- 0.6	135.0	48	V
28	- 0.2	-135.0	48	U

Table 4.2: Geometry Data of Upstream PCs

- Obtain the last recorded position and momentum of the decay positron: (u, v, z) and (p_u, p_v, p_z), directly from the trees in order to reconstruct its track back to $z =$ `zpulast_anal` cm (z-coordinate of `pulast_anal`). This must be done in order to find the number of decay positrons that "penetrate" the dead zone in `pulast_anal` vs. the number that actually "fire" a wire in that region.
- If the coordinates from this tracking are within a certain tolerance of the of the dead zone, we histogram this event as "penetrating" the dead zone.
- If the last recorded (u, v) for the decay positron are within a tolerance of the (u, v) fired by the incident muon, we histogram this event as "firing" in the dead zone.

4.4 The Tests

In order to determine whether or not the analysis code is working in a sane manor, it performs the following tests:

4.4.1 Trackswimming Test

- *If* the last u-plane hit was `pulast_anal`, *and* the last v-plane hit was `pvlast_anal`, *then*:

  (1) Histogram: $(u_{fit} - u_{data})$

Where u_{fit} is the u-coordinate of the trackswimming back to `pulast_anal`, and u_{data} is the u-coordinate recorded in data at `pulast_anal`.

(2) Histogram: $(v_{fit} - v_{data})$

Where v_{fit} is the v-coordinate of the trackswimming back to `pvlast_anal`, and v_{data} is the v-coordinate recorded in data at `pvlast_anal`.

This test has proved to be very useful. By looking at the two histograms, we can tell whether or not the code is behaving the way it should be. If both histograms show a sharp peak around zero, we know the trackswimming is consistent with data. A recent example of this is shown in figure (4.1).

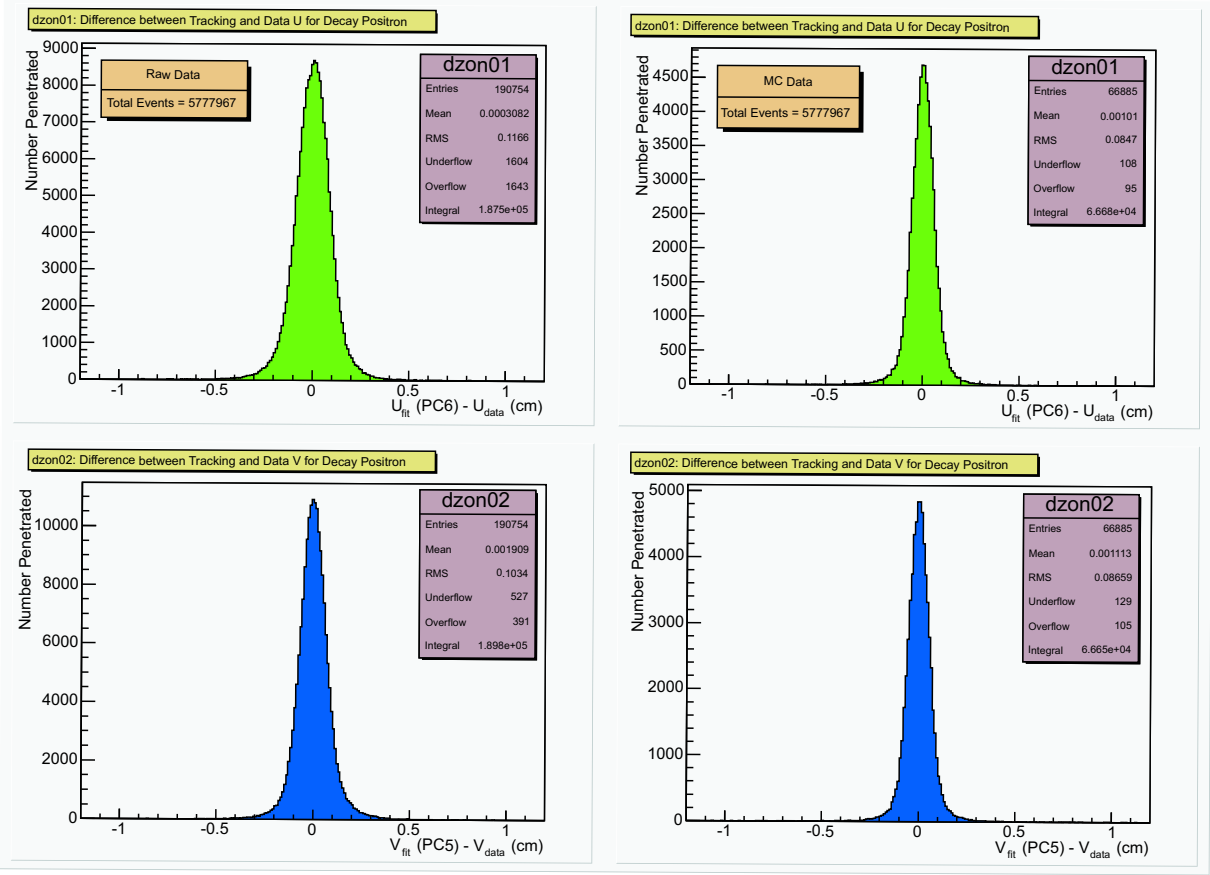

Figure 4.1: Trackswimming Test

In fact, this test showed that PC6 was misaligned by a small amount. It has now been implemented in the code to artificially shift all the relavent u-coordinates by $u_{shift} = 0.04678$ cm.

Notice, in figure (4.1), that the RMS in RD (Raw Data) is larger then that for MC (Monte Carlo) by about 38% in the u-direction, and about 17% in the v-direction.

4.4.2 Beam Spot Test

This is a simple test that confirms whether or not the muon beam spot from the M13 beamline is as it should be. Figure (4.2) shows two things:

(1) A projection of the beam spot on the u-axis of PC6 in terms of wire number. (Here $u = 0$ is half way between wires 80 and 81).

(2) A 2D projection of the beam spot using u-coordinates from PC6 and v-coordinates from PC5.

Both should be symmetric about their respective centers, and we can see the effect of the wires discretizing the coordinate values. On the beam spot, high numbers of counts occur only where two wires cross as illustrated by the color coded contour plot. However there are still some counts in between wires. This is because of the weighted average performed in the analysis of the wire chamber hits when more then one wire fires for the same event.

Basically we can check whether anything out of the ordinary is going on in this plot just by looking the the shape of the beam spot. `Root` tells us that the mean value in the v-direction is slightly off center, with a value of -0.3025. This is the way the beam spot is, it is known to be not perfectly symmetric. So we should expect an asymmetry in the decay positron hits along the v-direction because of this.

4.4.3 Dead Zone Test using u-coordinates

This is the first test performed to check whether the algorithm is working and shows indirect evidence of the dead zone.

On the left hand side of figure (4.3) is a stack of two histograms. The larger histogram is the number of positrons *penetrating* the dead zone, while the smaller one is the number of positrons that caused a wire to *fire* in the dead zone. Both are in terms of the wire number in PC6.

On the right hand side is the ratio: (number firing) / (number penetrating) histogrammed vs. wire number in PC6.

The constant value of this histogram is a measure of the probability for a positron to fire a wire when it penetrates the dead zone. About 45% of the time the positron will fire a wire, while the rest of the time, the wires don't fire at all.

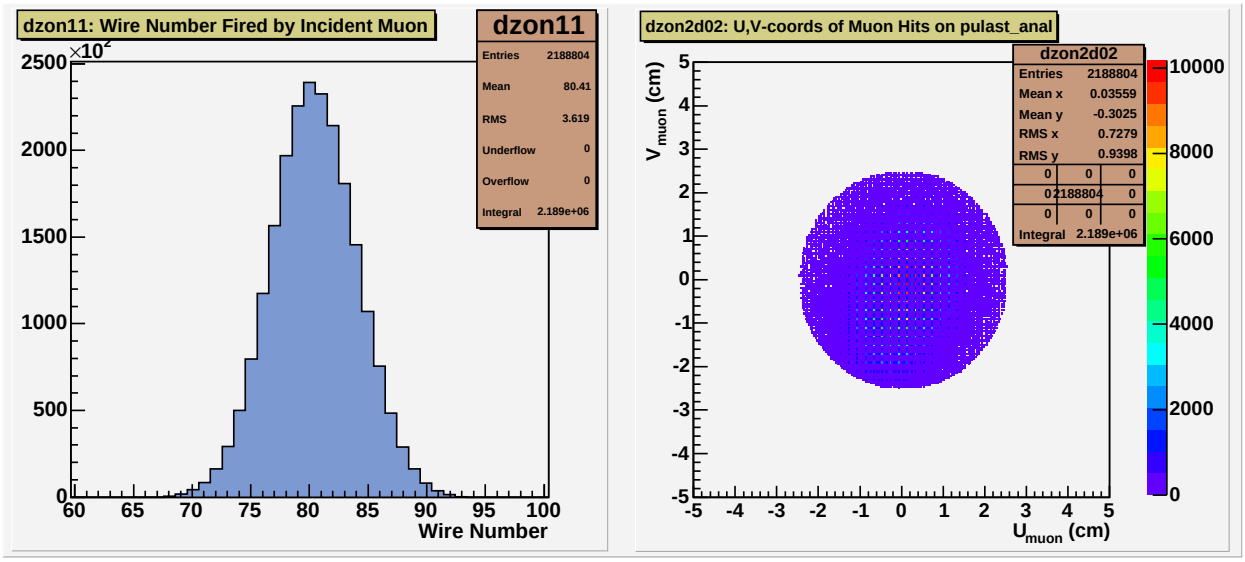

Figure 4.2: Beam Spot Test (dzon11 & dzon2d02) taken from RD Set2 / Anal22

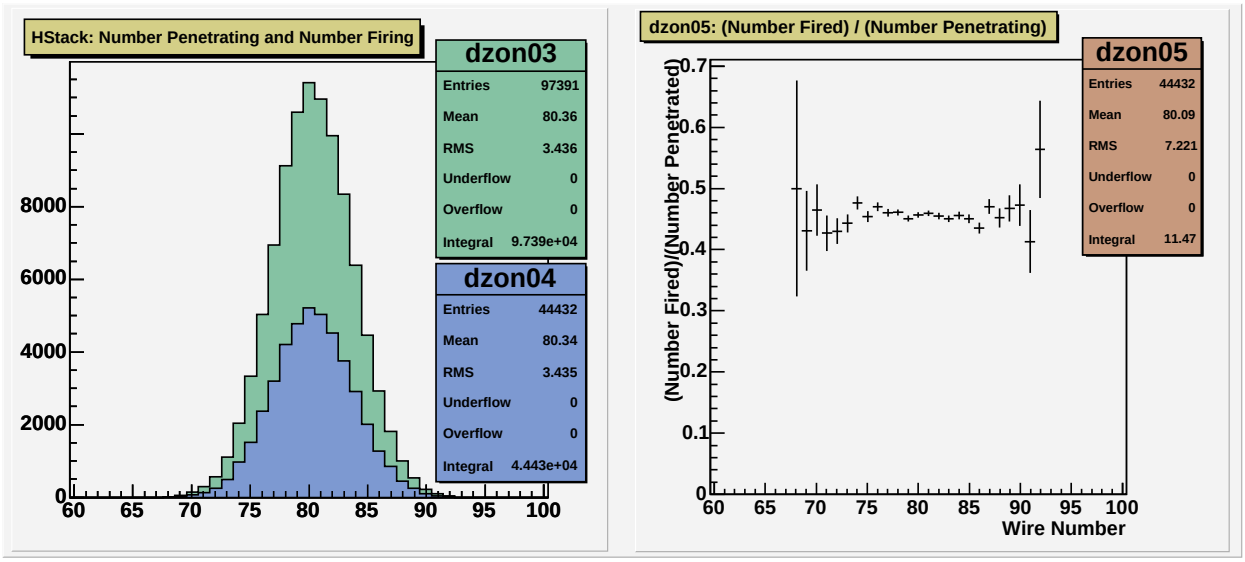

Figure 4.3: Dead Zone Test using u-coordinate (dzon03/dzon04 & dzon05 with error bars) taken from RD Set2 / Anal22

The error bars plotted here were calculated using equation (4.1):

$$\sigma = \frac{\sqrt{N(1-\frac{N}{T})}}{T} \tag{4.1}$$

Where:

- $N \rightarrow$ Number firing
- $T \rightarrow$ Number penetrating

4.4.4 Dead Zone Test using Window Times

Similar to figure (4.3), figure (4.4) contains the same histogram stack, except now in terms of window time (ns). The number penetrating the dead zone has an exponential decay rate characteristic of the muon lifetime: $\tau_\mu = 2197.03$ ns.

Also, the same ratio is plotted on the right hand side, which is also a measure of the probability for a positron to fire a wire when penetrating the dead zone. This probability increases with time, which makes sense, because the muon has less probability of creating space charges in wires as its decay time is reached. That is, less and less muons are present in the spectrometer as the window time increases because they have a decay time much shorter than the window duration.

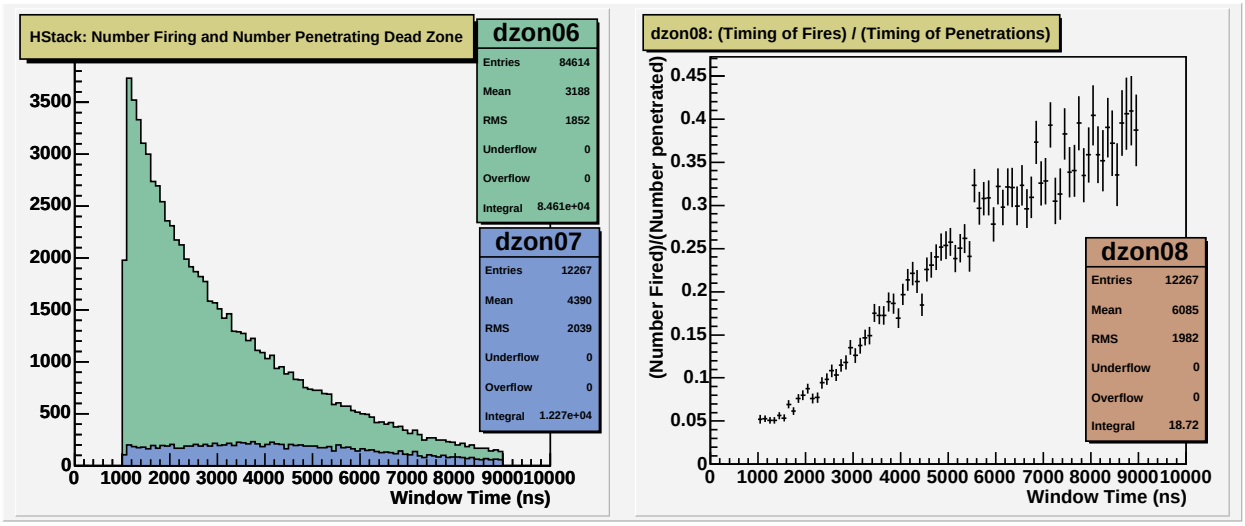

Figure 4.4: Dead Zone Test using Window Times (dzon06/dzon07 & dzon08 with error bars) taken from RD Set2 / Anal22

4.5 An Important Histogram

One of the most important histograms in this analysis is shown in figure (4.5). In order to find strong evidence of the dead zone, we histogrammed the number of positrons penetrating the dead zone against $(v_{fit} - v_{muon})$, where:

- $v_{fit} \rightarrow$ positron trackswimming v-coordinate in PC6
- $v_{muon} \rightarrow$ positron data v-coordinate in PC6

So, when the muon and the positron pass near the same v-coordinate along a particular wire, then: $v_{fit} - v_{muon} \approx 0$.

We then histogrammed the number of positrons actually firing the dead zone wire against the same variable, and histogrammed the same ratio: (Number Firing) / (Number Penetrating) with the correct error bars. These are shown in figure (4.5).

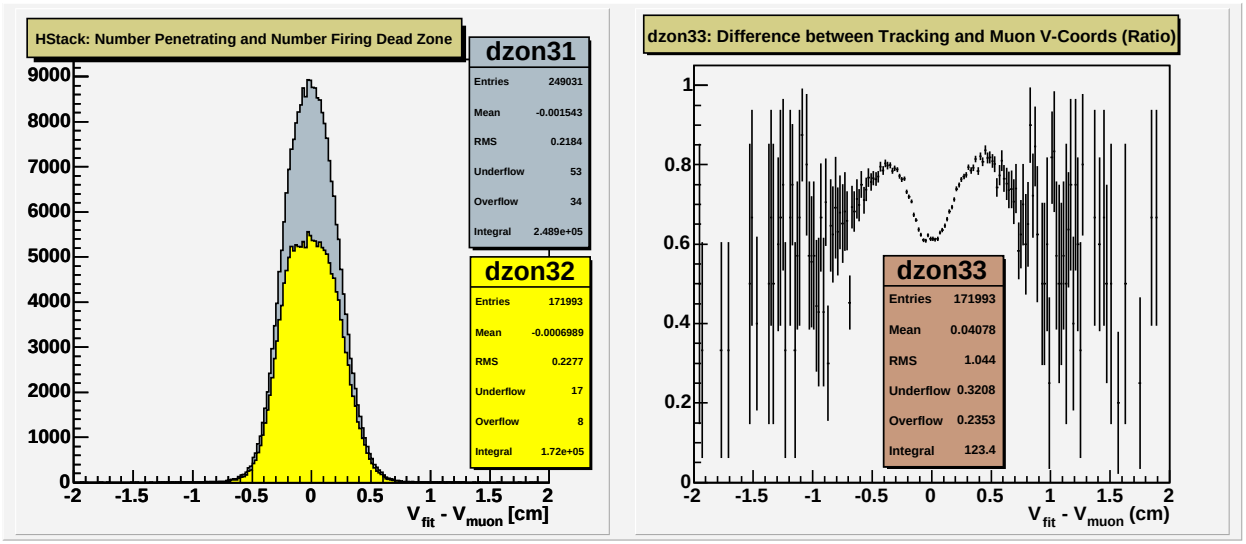

Figure 4.5: $v_{fit} - v_{muon}$ in PC6

Notice the significant "dip" occuring around $v_{fit} - v_{muon} = 0$. This shows strong evidence of the dead zone in PC6. The "dip" occurs around zero because this is where the muon and positron pass through the same region along the wire. If many positrons penetrate this region, but a significantly smaller number of them actually fire that wire, then the ratio of the two should produce a "dip". We will see later that the area in this dip contains information about the average length along the wire that is dead.

Next we filled a 2D histogram with all the ratio values for all the available window times: $1050 \leq t_{win} \leq 9000$ ns. (This operation required the use of the subroutine `T2DH_Divide()`, which divides one 2D histogram by another. There is not yet a function in `root` which performs this operation). Plotting this as a `lego2` plot in `root` gives the result shown in figure (4.6).

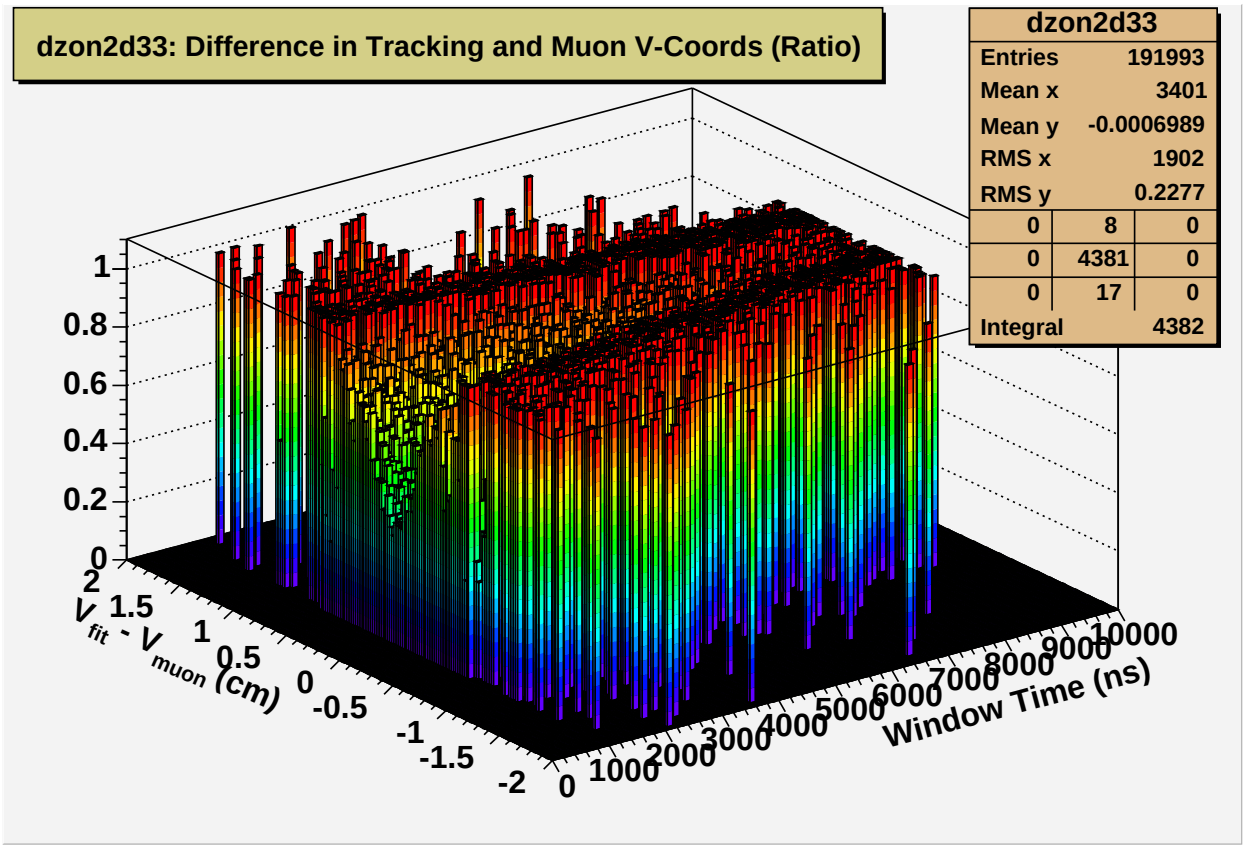

Figure 4.6: $v_{fit} - v_{muon}$ vs. Window Time in PC6

This 2D plot shows something similar to figure (4.5), infact if this plot were integrated over time the result you'd get is that in figure (4.5). Here we can see that the "dip" changes over time, it gets less and less deep as time increases.

The next step is to look more closely at these two plots, and try to get some useful information out of them. Maybe the time-dependence of the "dip" can tell us about the *healing* time of the dead zone.

4.6 The Fitting

How can we get information about the dead length and healing time out of the dead zone plot in figure (4.6)? One way is to fit the data using the standard *MINUIT* least squares fitter with some predefined function. It just so happens that *ROOT* contains this fitter, and a macro has been written a to fit the dead zone histogram in figure (4.6) with the following

function:

$$Z(x,t) = -\frac{A_o}{\sqrt{2\pi}\sigma} \exp\left[-\frac{(x-\alpha)^2}{2\sigma^2} - \frac{t}{\tau_h}\right] + \xi \tag{4.2}$$

Where:

- $x \rightarrow (v_{fit} - v_{muon})$
- $t \rightarrow t_{window}$
- $A \rightarrow$ parameter; Gaussian amplitude (negative)
- $\tau_h \rightarrow$ parameter; Dead zone healing time
- $\alpha \rightarrow$ parameter; Offset from $x = 0$
- $\sigma \rightarrow$ parameter; Gaussian RMS
- $\xi \rightarrow$ parameter; Offset from $Z = 0$

(The motivation for using this function will be explained later).

We then hypothesize that the parameter A in this function is related to the dead length L_{dead}. But how can we find this relation?

The answer can be found by using Monte Carlo simulations of the experiment. Suppose, in the simulation, we implemented a dead zone based on knowledge of its effect, then ran a few million events to analyze with my "Deadzone" code. How can we get back out of the analysis what we put in as the L_{dead} value?

In the Monte Carlo program, the dead zone is approximately represented by a square well, that is, a ratio histogram from MC similar to figure (4.5) is almost a square well when put into the simulation. But, since the experiment is measured with limited resolution, measuring the simulated data with the "deadzone" analysis code gives a smeared result. This can be described using convolution theory.

Recall the definition of a convolution, given by equation (4.3):

$$C(x) \equiv s * g = \int_{-\infty}^{\infty} s(t)g(x-t)dt \tag{4.3}$$

If $s(x)$ is the original function (square well), and $g(x)$ is the smearing function (normalized Gaussian), then the convoluted function is $C(x)$.

Let $s(x)$ and $g(x)$ be defined by equations (4.4) and (4.5):

$$s(x) = \begin{cases} \xi & \text{if } |x| > L/2 \\ 0 & \text{if } |x| \leq L/2 \end{cases} \tag{4.4}$$

$$g(x) = \frac{A}{\sqrt{2\pi}\sigma} \exp\left(\frac{-x^2}{2\sigma^2}\right) \tag{4.5}$$

Then it can be shown that the convolution of $s(x)$ with $g(x)$ is given by equation (4.7):

$$C(x) = \frac{\xi A}{2}\left[\text{erfc}\left(\frac{x+L/2}{\sqrt{2}\sigma}\right) - \text{erfc}\left(\frac{x-L/2}{\sqrt{2}\sigma}\right) + 2\right] \tag{4.6}$$

$$= -\frac{\xi A}{\sqrt{\pi}}\int_a^b e^{-t^2}dt + \xi A \tag{4.7}$$

Where:

- $a = \frac{x-L/2}{\sqrt{2}\sigma}$
- $b = \frac{x+L/2}{\sqrt{2}\sigma}$

and $\text{erfc}(x)$ is the complementary error function, defined by:

$$\text{erfc}(x) \equiv 1 - \text{erf}(x) = \frac{2}{\sqrt{\pi}}\int_x^\infty e^{-t^2}dt \tag{4.8}$$

It is now clear that this particular convolution is quite complicated, and cannot be reduced from its integral form. Under certain conditions, it can be approximated by a Gaussian with a negative amplitude. As shown in figure (4.7), there are two extremes to equation (4.6): one is when $\sigma \ll L$, the other is when $\sigma \gg L$.

On the top, for $\sigma \ll L$, the curve shape is dominated by the two error functions *individually*, that is, they sum in regions of x where their values are small. Thus the curve is *not* dominated by the sum of the error functions.

However, on the bottom, for $\sigma \gg L$, the curve shape *is* dominated by the sum of the two error functions. The result is something that can be approximated by a Gaussian with a negative amplitude. This is the case we are most interested in. There is no reason why this function cannot be fit by an error function, but it is considerably simpler to model it with a Gaussian as described.

We want to use the "conservation of area under the curve" property of convolutions in our analysis. If the area under the curve of the square well function $s(x)$ is equal to that of the convoluted function $C(x)$, then the area inside the "dip" of $s(x)$ is also equal to the area inside the dip of $C(x)$, which is no longer square and impossible to integrate analytically. But if we approximate $c(x)$ with a Gaussian, it becomes rather simple to find a relation between the length of the dead zone that is input in the Monte Carlo, and the amplitude we measure upon analysis.

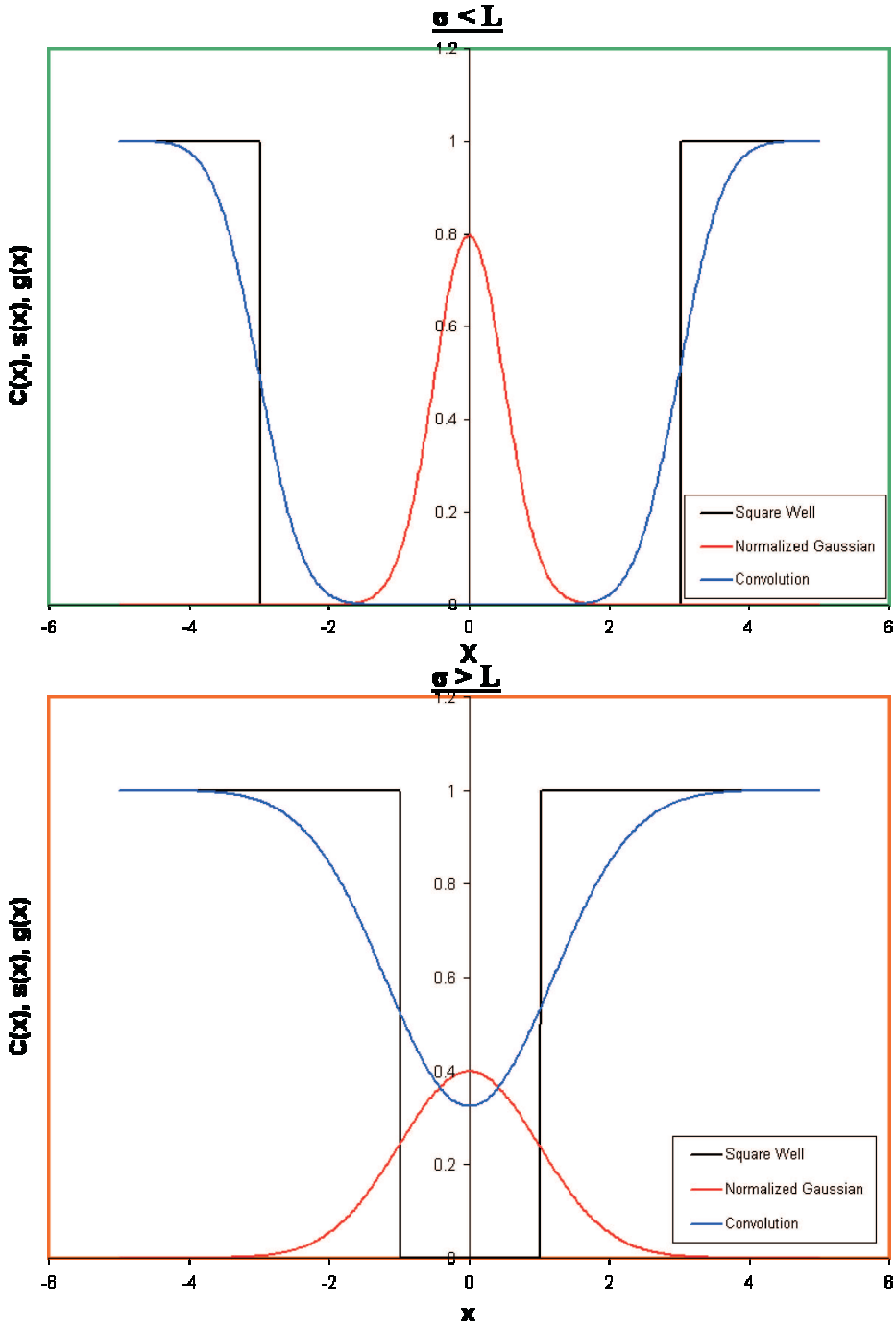

Figure 4.7: Two extremes of $C(x)$

Using the conservation of area property of convolutions, we can equate the following two expressions:

$$\int_{-\infty}^{\infty} \hat{s}(x)dx \quad = \quad \xi L_{dead} \tag{4.9}$$

$$\int_{-\infty}^{\infty} \hat{C}(x)dx \;\approx\; \int_{-\infty}^{\infty} \frac{A_o}{\sqrt{2\pi}\sigma} \exp\left(-\frac{x^2}{2\sigma^2}\right) dx = A_o \tag{4.10}$$

Where:

- $\hat{s}(x) = \xi - s(x)$
- $\hat{C}(x) = \xi - C(x)$

When equations (4.9) and (4.10) are equated we obtain a very simple relation between the dead length L_{dead} and the amplitude of the convolution A_o:

$$L_{dead} = \frac{A_o}{\xi} \tag{4.11}$$

This result can be implemented into our fitting function, from which we can calculate the dead length directly. The result is given by equation (4.12):

$$Z(x,t) = -\frac{\xi L_{dead}}{\sqrt{2\pi}\sigma} \exp\left[-\frac{(x-\alpha)^2}{2\sigma^2} - \frac{t}{\tau_h}\right] + \xi \tag{4.12}$$

The motivation for using this function now becomes quite evident. We use a normalized Gaussian with a negative amplitude along the x-direction, and we hypothesize that the "dip" *heals*, or grows, exponentially. Hence the e^{-t/τ_h} factor. Let's see how well this function fits the "Deadzone" histogram shown in figure (4.6).

Chapter 5

Results

Using my "Deadzone" analysis code on PC6 with about 1.6×10^7 events in SET2 / ANAL22, we find the following results when fit with ROOT:

Parameter	Value	Error
L_{dead}	0.4811 cm	$\pm$0.0050 cm
τ_h	2444 ns	$\pm$41 ns
α	-0.00063 cm	$\pm$0.00137 cm
σ	0.2094 cm	$\pm$0.0027 cm
B	0.8953	$\pm$0.0028
χ^2	ndf	χ^2/ndf
5109	3864	1.322

Table 5.1: Results for Fitting Dead Zone in PC6

Figure (5.1) shows the function the parameters in table (5.1) describe.

The ratio of the χ^2 over the number of degrees of freedom (ndf) are close to one. This suggests that both fits to the dead zones in PC5 and PC6 were done reasonably well.

The size of the dead zone in PC5, as characterized by the dead length L_{dead}, is smaller than that in PC6 by about 50%. The healing time τ_h is also smaller by about 25% in PC5 as compared to PC6.

This is expected because the muon deposits more energy in the wire chamber closer to its decay vertex, thus creating the larger dead zone. Since PC6 is closer to the target, and therefore the average position of muon decay, the dead zone there is larger than in PC5, behind it. Larger dead zones have a larger L_{dead} and a longer τ_h. So the results found agree

Parameter	Value	Error
L_{dead}	0.2630 cm	$\pm$0.0117 cm
τ_h	1856 ns	$\pm$82 ns
α	0.0170 cm	$\pm$0.0023 cm
σ	0.1064 cm	$\pm$0.0021 cm
B	0.8794	$\pm$0.0014

χ^2	ndf	χ^2/ndf
4385	4988	0.8791

Table 5.2: Results for Fitting Dead Zone in PC5

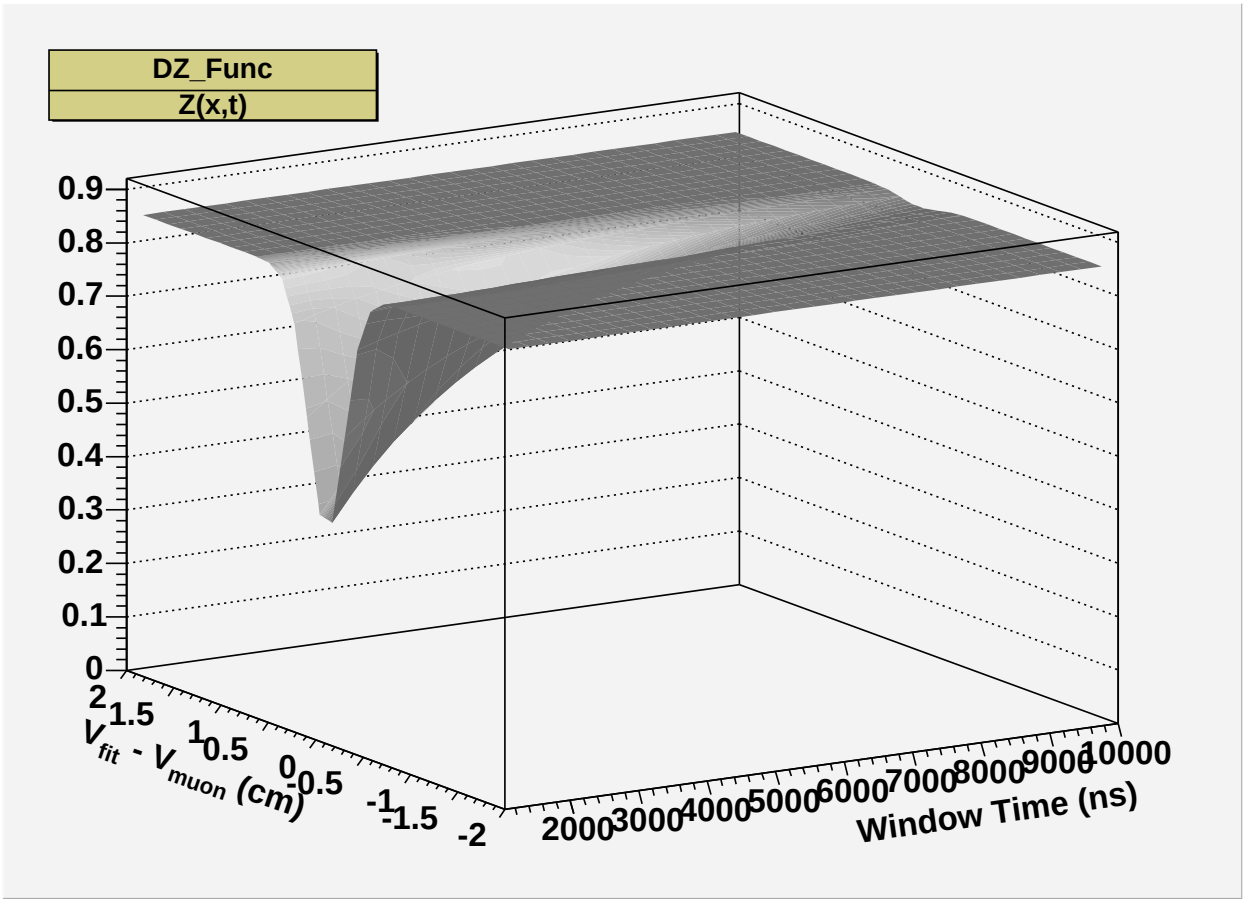

Figure 5.1: Fitting function $Z(x,t)$

with the theory.

5.1 The Scaling Factor

In order to measure the uncertainty that the dead zone creates with respect to the Michel parameters, the use of Monte Carlo simulation is needed yet again. The scaling factor is a convenient way to measure this quantity.

Suppose we have a measurable quantity R that depends on another variable x for which the uncertainty is known. We wish to find the systematic uncertainty of R. Then the scaling factor, S, is defined as:

$$S = \frac{x_{MC}}{x_{RD}} \tag{5.1}$$

Where:

- $x_{RD} \rightarrow$ value found in raw data creating the quantity $R(x_{RD})$
- $x_{MC} \rightarrow$ value input into Monte Carlo analysis which is to exagerate the effect of $R(x_{RD})$ in raw data

Then the systematic uncertainty of R is given by:

$$\sigma^2_{sys}(R) = \frac{1}{S^2}\left(\Delta R^2 + \sigma^2_{\Delta R}\right) \tag{5.2}$$

Where:

- ΔR is the central value result of a fit done on the difference between a normal Monte Carlo data set (with no dead zone) and a Monte Carlo data set with a dead that exagerates that in real data.
- $\sigma_{\Delta R}$ is the statistical uncertainty on the central value obtained from the fit.

In our analysis, the variable x is equivalent to the number of counts lost due to the dead zone. So we create a simulation with an exagerated dead zone, where the number of counts lost will be a lot more than in real life (raw data).

The dependent variable $R(x)$ is then the value of any one of the Michel parameters: ρ, δ, η, or ξ. And $\sigma^2_{sys}(R)$ is the systematic uncertainty of a Michel parameter associated with the number of counts lost due to the dead zone.

Unfortunately, the Monte Carlo has not yet been fully debugged and the results it gives for the dead zone are not yet satisfactory. Until it has been fully debugged, this study cannot be completed.

Chapter 6

Discussion and Conclusion

In summary of this dead zone study, we can now answer the questions that were posed as motivation for performing it:

(1) How large is the dead zone on average?

In PC5: $L_{dead} = 0.2630 \pm 0.0117$ cm

In PC6: $L_{dead} = 0.4811 \pm 0.0050$ cm

(2) How long does it take for the dead zone to "heal"?

In PC5: $\tau_h = 1856 \pm 82$ ns

In PC6: $\tau_h = 2444 \pm 41$ ns

(3) What is the probability that a positron will go through the dead zone without firing the corresponding wire?

There is not one answer to this question, because this probability is time dependent. A more relavent question would be: what is the probability that a positron will go through the dead zone without firing its corresponding wire at a time t_o ?

This question can be answered by fitting the histogram shown on the right hand side of figure (4.4) with a straight line:

$$P(t) = at + b \tag{6.1}$$

For $1000 \leq t_o \leq 9000$ ns. The fit parameters we found to be:

- $a = (5.032 \pm 0.070) \times 10^{-5}$ s^{-1}
- $b = (-0.01645 \pm 0.00195)$

So, for example, at a time half way through the event window: $P(4000\text{ ns}) = 0.185 \pm 0.003$. Where the uncertainty in the probability is given by:

$$\delta P(t) = \sqrt{(\delta a)^2 t^2 + (\delta b)^2} \tag{6.2}$$

But this is a measure of the probability that a positron *will* fire a wire in the dead zone, so the probability that the positron *will not* fire a wire in the dead zone is: $1 - P(t) = 0.815 \pm 0.003$.

(4) What effect does this dead zone have on the analysis of the Michel parameters? Ie; what is the systematic uncertainty of the dead zone effect?

As mentioned in §5.1, there is still some debugging to do in the Monte Carlo simulation code. Until that has been completed this question cannot be completely answered.

Some rough estimates of the systematic error for the dead zone have been calculated to be 0.00×10^{-3}. If these results prove accurate, once a proper calculation can be done, then the dead zone systematic will have little to no effect on the Michel parameters.

At present, the *TWIST* group is very close to publishing their first results of the Michel parameters to the 10^{-3} level. In order to ensure that this experiment can continue on to the 10^{-4} level, they must be sure that their systematics are lower than a few parts in 10^5. Otherwise the Michel parameters will be limited by the systematics of the experiment.

This dead zone study will add another value to the table of systematics that the experiment has already accumulated. But on top of that, this study has shown evidence of a time dependence on the efficiency of proportional counters when dealing with large energy loss. When using a muon beam where the muons are incident on the spectrometer at some rate, the creation and destruction of a dead zone near the end of the muon lifetime will be periodic *only if* the healing time of the dead zone is less than the period of incident muons (1/rate).

In fact, it would be even better to have an incident muon every three or four times τ_h, because the healing time is really the time it takes for *half* of the dead zone to heal. Think of it as a decay time for an ensemble of radioactive particles.

If τ_h is larger than the period of incident muons, the dead zone will essentially be there forever. This is not good for the efficiency of the proportional chambers, because they will continually lose hits. There is even a chance of the dead zone growing to the size of the entire chamber plane, if the rate of muon incidence is large enough. Muons that continually bombard the PC without enough time for the ions to recombine with the electrons will cause the dead zone to grow, until the space charge inside the PC reaches some upper limit.

This subject has not been thoroughly studied enough to confirm this theory. Further studies on dead zones should be done using Monte Carlo simulations of single multi-wire proportional counters. This kind of research might be performed by myself over the next year as an undergraduate thesis.

Bibliography

[1] W. R. Leo: *Techniques for Nuclear and Particle Physics Experiments: A How-To Approach*, 2nd Ed. (1994), p.127 - 156

[2] W. Riegler: *Limits to Drift Chamber Resolution*, (1997), p.76 - 80

[3] W. H. Press ... [et. al]: *Numerical Recipes in C: The Art of Scientific Computing*, 2nd Ed. (1992), p.220

[4] R. Brun ... [et. al]: *ROOT: Users Guide 3.10*, (2003)